Damage of TWIP Steels for Automotive Application

J.Lorthios,[1] A.F.Gourgues, P.Cugy, C.Scott [2]
[1] Centre des Matériaux ENSMP, Evry, France;
[2] ArcelorMittal, Maizières-lès-Metz, France;
E-mail: *julie.lorthios@ensmp.fr*

1   Introduction

Ultra high strength Fe-Mn-C austenitic steels with low Stacking Fault Energy (SFE) have been studied for more than fifty years [1]. They offer a great potential for reducing automotive body weight through their formability and their high mechanical properties. Tensile strength levels higher than 1000 MPa in combination with a high ductility (>50%) are reached by the optimization of the Twinning Induced Plasticity (TWIP) effect and the control of the microstructure.

However, the combination of plastic instabilities and the TWIP effect can lead to unusual macroscopic behaviour. Fe-Mn-C steels break with atypical failure modes, e.g. in uniaxial tension, no necking is observed whereas the fracture surface is fully ductile. Thus standard forming limit curve based analyses cannot be applied to these materials.
The deformation mechanisms of such steels are reasonably well known. The present work gives an additional contribution concerning damage and rupture. The damage and rupture mechanisms of thin sheets of ultra high strength Fe-Mn-C TWIP austenitic steels have been investigated.

The first approach focuses on the determination of a macroscopic failure criterion (strain, stress or localization criterion). To this aim, specific experiments are conducted in order to test the material in loading modes closer to those encountered during real forming processes, such as deep drawing.
Loading material along the thickness direction is usually difficult for thin sheets. Such a loading mode can be studied with shear cutting experiments ([2], [3]). Among the interesting results is the crack path because it strongly depends on both the hardening capacity of material and its sensitivity to strain localization. Strain and stress fields during shear cutting will be determined by FE calculations in order to interpret the results of such an experiment. FE calculations need in turn simple experiments on smooth, U-notched and Kahn specimens to establish the constitutive equations of the steels. In this paper, the full experimental basis for this approach is established.

The second objective of the study is to investigate damage mechanisms in relation to the deformation microstructure. The aim of this approach is to obtain information about damage initiation (cavities localized at grain boundaries, at the intersection of grain boundaries and twins or of two twins) and fracture mechanisms at the microscopic scale. Up until now these mechanisms are not known. As a first step, interrupted experiments on Kahn

and shear cutting specimens were conducted to obtain stopped cracks and damage beyond the crack tip was observed.

2   Experimental procedures

2.1   Material

The plasticity mechanisms of austenitic Fe-Mn-C steels (dislocation glide, mechanical twinning and phase transformations) are governed by the value of the SFE which depends on the chemical composition and temperature (Figure 1). Thus the composition has a major influence on the mechanical properties of these alloys.
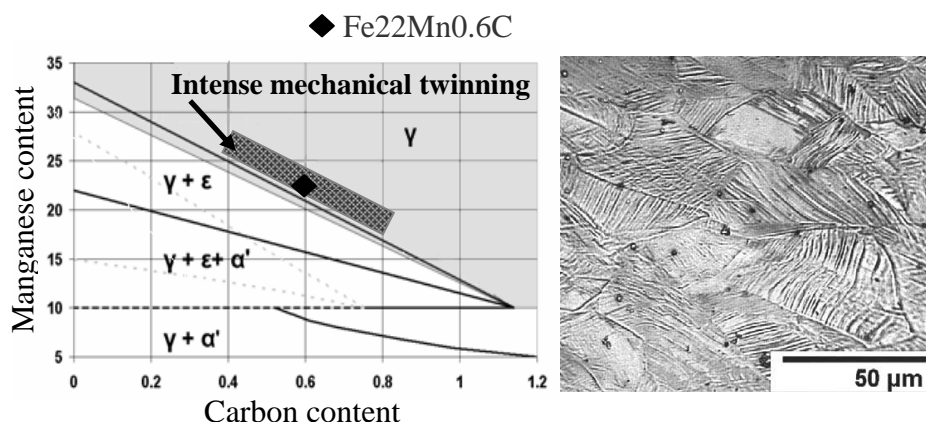

Fig2. Phases stability after deformation at room temperature depending on manganese and carbon content [1]

Fig3. Optical micrograph after etching to reveal grain boundaries and twins from a sample deformed at 293K [2]

The study focuses a recrystallized Fe-Mn-C steel sheet of 1.5mm in thickness, containing 0.6% of carbon and 22% of manganese. The grain size is 2-3µm.
The composition of the steel under investigation was optimized to exhibit a low SFE in order to keep the austenitic phase stable during plastic deformation. This low value promotes mechanical twinning (Figure 2) - in competition with planar dislocation glide - as main deformation mode, inducing a TWIP (Twinning Induced Plasticity) effect. The increasing density of twins with strain reduces the mean free path of dislocations because twins act as obstacles. It results a high hardening rate. Relaxation mechanisms inside twins promote a high elongation capacity before fracture.

2.2   Experiments

All experiments were carried out at room temperature and have been duplicated. As experiments were highly reproducible, only one curve is given for each testing condition.

Tensile tests on smooth, U-notched and Kahn specimens were used to characterize the mechanical behaviour of the Fe22Mn0.6C steel.

Specimens were loaded along rolling (R), long transverse (T) and diagonal (45 between R and T) directions to examine any anisotropy effect on mechanical characteristics and fracture surfaces.

Experiments on smooth specimens were carried out at $4.10^{-4} s^{-1}$, $4.10^{-3} s^{-1}$ and $4.10^{-2} s^{-1}$ to estimate the strain rate sensitivity of the steel under quasi-static conditions. Tensile tests on U-notched specimens were performed for various notch radii to investigate the effect of stress triaxiality on the mechanical behaviour of the Fe22Mn0.6C steel. Three notch radii were selected (r=0.5, r=1 and r=2) leading to different levels of triaxiality (typically between 1/3 and 2/3).

Cracking resistance was studied with Kahn specimens, which induce stable crack growth due to mixed tensile and bending loading conditions. Crack initiation and propagation energy were measured from tearing curves.

Shear cutting experiments were realized with an in-house assembly mounted on a tension-compression testing machine. Bands of 5 mm in thickness have been tested at a blade displacement rate of 1 mm/s with a clearance between blades of 6% of the sheet thickness.

Interrupted experiments on Kahn and shear cutting specimens were performed in order to study damage mechanisms. The other specimens were examined after fracture. Fracture surfaces and cross-sections of stopped cracks were observed by scanning electron microscopy (FEG-SEM).

3   Results: Flow behaviour

Figure 3 illustrates the stress-strain behaviour of the Fe22Mn0.6C steel at $4.10^{-3} s^{-1}$ along R, T and 45 directions. The results reveal an ultimate tensile stress higher than 1000MPa and a uniform elongation up to 50%.
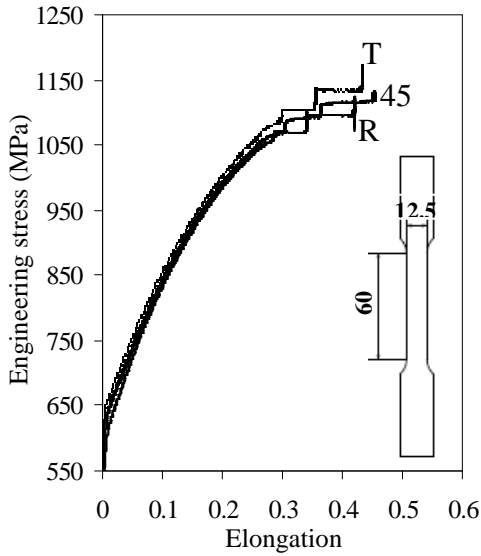
Fig3. Engineering stress – strain in tension ($\dot{\varepsilon}$=4.10⁻³s⁻¹) of Fe22Mn0.6C steel along rolling (R), transverse (T) and diagonal (45) directions.
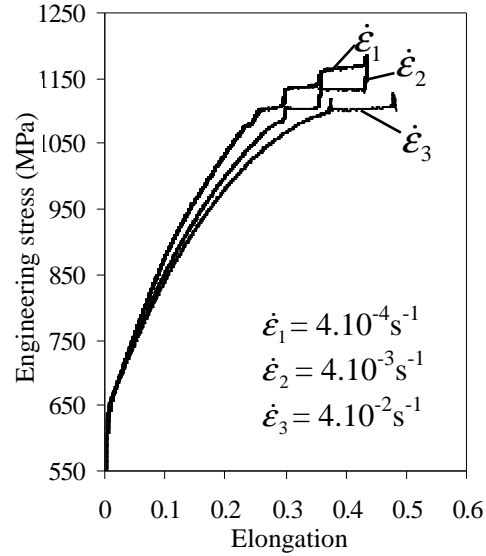
Fig4. Engineering stress – strain in tension of Fe22Mn0.6C steel along transverse direction (T) for three strain rates. Same specimen geometry as in Fig. 3.

The mechanical properties of Fe22Mn0.6C are near-isotropic. Lankford coefficients measured directly on the specimen after fracture (far from the necking area), corroborate this result (Table 1).

	Lankford coefficients
R specimen	0.95
45 specimen	1.20
T specimen	1.35

Table1. Lankford coefficients measured on specimens after fracture loading along rolling (R), transverse (T) and diagonal (45) direction.

The Fe22Mn0.6C steel exhibits negative strain rate sensitivity in quasi-static testing conditions as illustrated in Figure 4. Furthermore serrations in curves are observed. Negative strain rate sensitivity and jerky flow are two characteristics of dynamic strain ageing due to pinning effect of solutes at moving dislocations. However S.Allain [2] measured a weak value of activation energy (13 kJ.mol⁻¹) for this phenomenon which cannot be attributed to a classical Portevin-Le Châtelier effect based on C diffusion to dislocations.

Tensile tests on U-notched (Figure 5) and Kahn specimens (Figure 6) and shear cutting experiments (Figure 7) showed the same small effect of anisotropy on the mechanical characteristics as for the smooth tensile specimens.

No serrations were observed on the tensile curves of the U-notched specimens because notches localize deformation in the notched area (Figure 5). Surprisingly, no notch strengthening effect was observed. The level of triaxiality seems to only influence fracture i.e. notch opening at rupture. This result is atypical with regard to other materials and will be interpreted in more details by FE calculations in the next future.
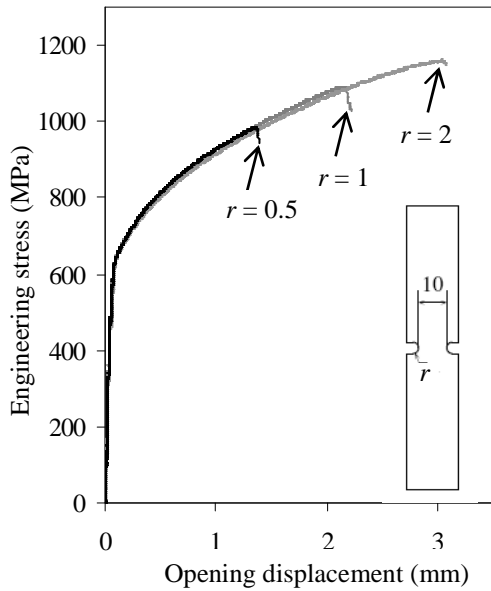

Fig5. Engineering stress – opening displacement on notched specimens loaded along the rolling direction.
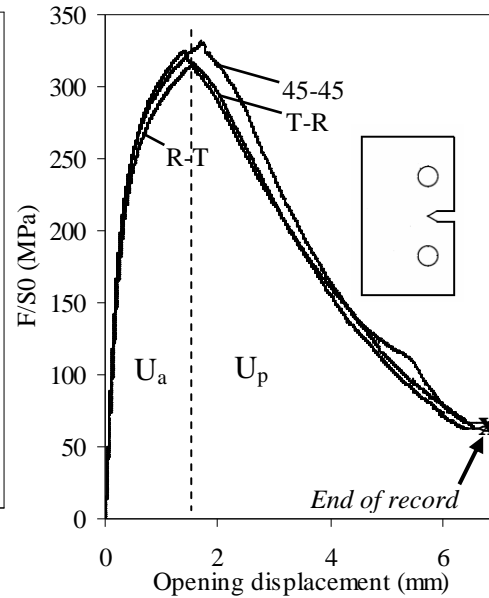
Fig6. Experiments on Kahn specimen loaded along rolling (R-T), transverse (T-R) and diagonal (45-45) directions.

Tearing curves of Kahn specimens present a sudden decrease in load as soon as the crack is initiated (Figure 6). Then, crack propagation remains stable up to fracture. The resistance to tearing can be defined as the surface area under the curves of Figure 6. These values are related to the energy dissipated in the initiation and propagation process of the crack respectively. The initiation energy U_i was calculated from 0 mm up to the initiation of cracking (at the maximum of the load). The propagation energy U_p was measured from the maximum of the load up to 7 mm, which corresponds to the opening limit of the extensometer. Table 2 gives values of these energies for the Fe22Mn0.6C steel.

	U_i (J/mm²)	U_p (J/mm²)	U_t (J/mm²)
T-R	0.44	1.35	1.78
45-45	0.44	1.18	1.63
R-T	0.40	1.28	1.69

Table2. Initiation, propagation and total energy U_i, U_p, U_t for a crack extension along R, T and 45° directions between 0 and 7 mm.

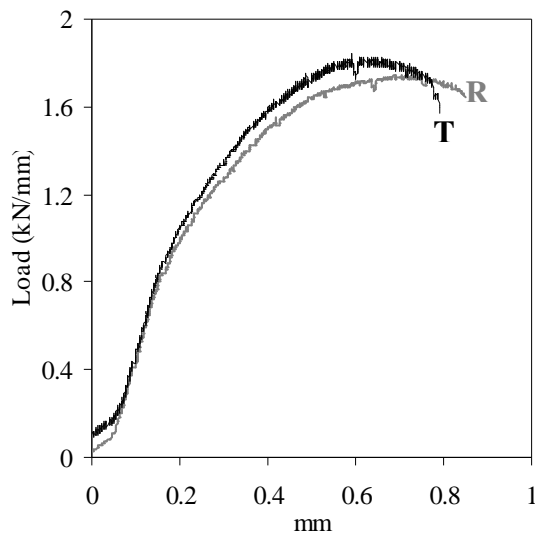Figure 7 illustrates the load per unit width of cutting sheets vs relative displacements of the blade.

Fig7. Shear cutting load per unit width (kN/mm) – displacement of the blade for specimens loaded along rolling (R) and transverse (T) directions.
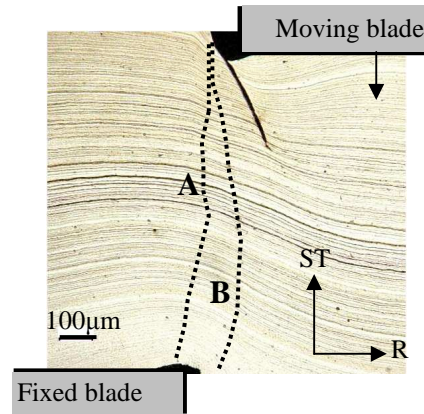

Fig8. Optical micrograph of interrupted shear specimen of Fe22Mn0.6C steel. Crack path of a Dual Phase steel (Profile A) and a 2024 aluminum alloy (Profile B) are indicated from [2].

Serrations on shear cutting curves are linked to the machine noise. Interrupted shear cutting experiments were carried out. Sample were polished in cross-section to observe the crack paths (Figure 8).

The crack path presents a convex trajectory in the shear cutting direction.

Other authors have carried out similar shear cutting tests with similar experimental conditions on a variety of materials ([2], [3]) including:

- a Dual Phase steel with high hardening capacity ($R_{p0.2}$=525MPa, R_m=858MPa, Elongation=21%; although less than that of TWIP steels) and not very sensitive to strain localization (Profile A in Figure 8). The crack path clearly goes toward the fixed blade in agreement with FE calculations. Here fracture is caused by decohesion of α'-martensite - ferrite interfaces followed by cavity growth and ductile fracture.
- Aluminium alloys with lower hardening capacity and marked sensitivity to strain localization (e.g. 2024 T351 $R_{p0.2}$=240MPa, R_m=441MPa). This material shows a convex crack path too (Profile B Figure 8), yet different from that observed in our study.

In comparison, the crack path of the Fe22Mn0.6C specimen is atypical in regard with the mechanical characteristics of the steel. The material presents both a high hardening rate and a high sensitivity to strain localization. FE calculations will allow determination of local stresses and strains and derivation of a fracture criterion to explain the crack path of the material.

4   Fracture behaviour

Smooth, U-notched and Kahn tensile specimens show the same fracture appearance, i.e. fracture with a 45° angle in thickness with respect to the loading direction (Figure 9). No localized necking is observed, except very close to the fracture surfaces. These characteristics are typical of slant fracture in ductile sheet metals ([5], [6], [7]). This behaviour has already been reported for materials which favour shear localization by low hardening rate or even softening effects. TWIP steels present a high hardening capacity and a very heterogeneous deformation mode (propagation of localized deformation bands [8]). Mechanisms such as dynamic strain ageing or TWIP effect could possibly explain the slant character of the fracture for this steel family.

45° angle in thickness

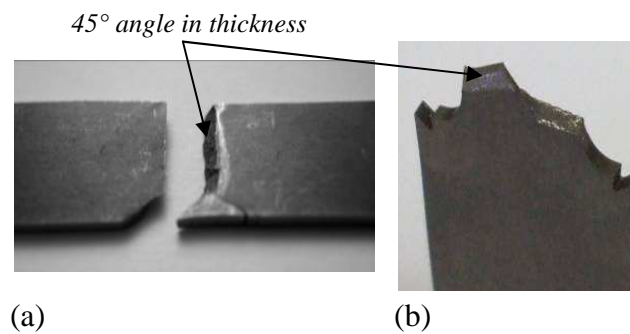(a)   (b)

Fig9. Fracture surface of (a) smooth and (b) U-notched specimens loaded in tension, showing slant fracture.

SEM micrographs of fracture surfaces of tensile specimens loaded along rolling, transverse and diagonal directions reveal ductile fracture (Figure 10). Deep and apparently empty voids have been observed. They are preferentially elongated along the rolling direction, whatever the loading direction revealing an anisotropic character of the fracture mechanisms.

The steel under investigation contains very few inclusions such as MnS precipitates which cannot explain the fracture surface appearance. Only a few cavities were observed in cross section views below the fracture surfaces, despite the presence of coarse cavities on the fracture surfaces. The segregation lines of C and Mn elements (visible in Figure 8 with appropriate etching solution) and the orientation of grains (whether clusters of grains of similar orientation exist or not) might be another explanation of fracture surface apearance. EBSD maps will allow the measurement of orientation clustering but the metallographic preparation is difficult and still in progress.

This fracture appearance has also been observed on the U-notched, shear cutting and tearing specimens with the same anisotropic dependence. The fracture surface depends on the material and on its orientation with respect to loading but not much on stress triaxiality.
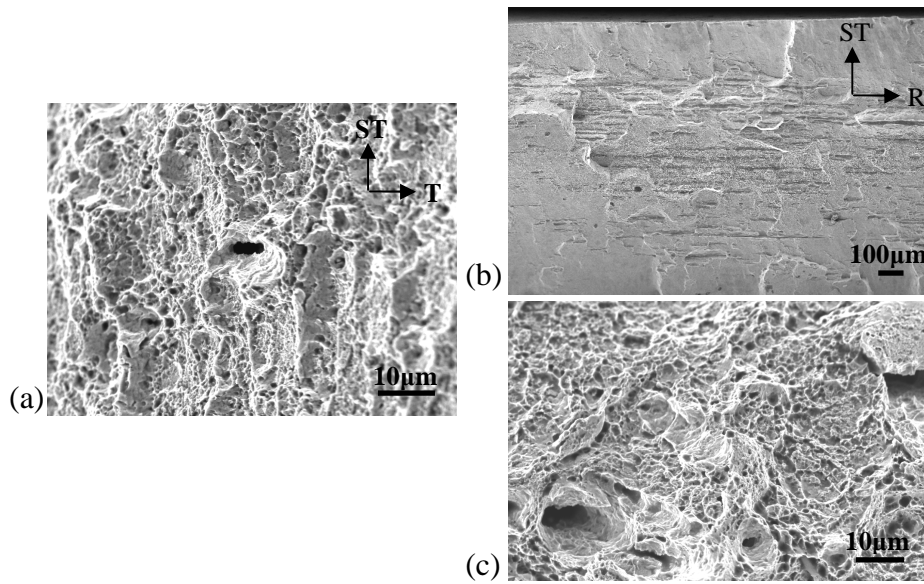
Fig10. Fracture surfaces of tensile specimens loaded along (a) rolling, (b) transverse and (c) diagonal directions on Fe22Mn0.6C steel.

Interrupted tests were used to analyse the microscopic aspects of deformation and damage by SEM observations (Figure 11). The crack tip seems to be somewhat blunt. Only little damage beyond it was observed. Microvoids are localized beyond the crack tip and along the crack lips.
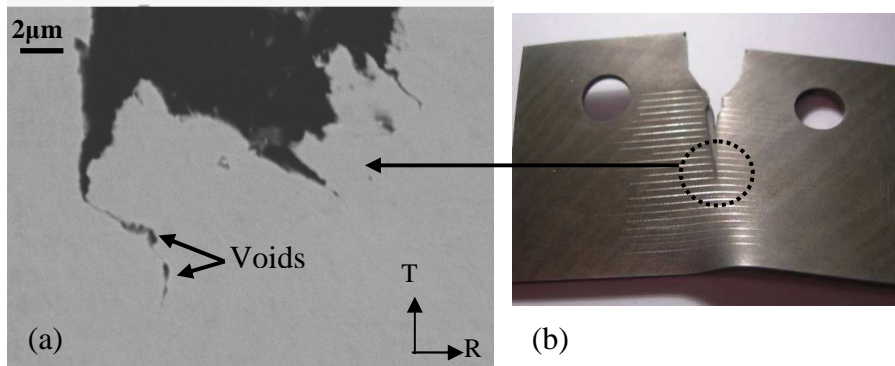

Fig11. SEM micrograph (a) showing damage beyond the crack-tip of an interrupted Kahn specimen (b).

The deformation microstructure has not been revealed by classical metallographic preparation (chemical etching after polishing). Ion polishing must be used to avoid artefacts from metallographic preparation for cavity observation. With this technique the localization of microvoids in regard with the deformation microstructure will be made possible.

5 Conclusions and future work

The mechanical behaviour of a Fe22Mn0.6C TWIP steel showed a negative strain rate sensitivity under quasi-static loading, a near-isotropy of flow properties and serrations on smooth tensile curves. No notch strengthening effect was measured. Only the fracture elongation was influenced by the stress triaxiality ratio. The steel under investigation reveals a high hardening capacity and strongly localizes deformation. It presents a high sensitivity to shear localization before fracture.

From these data, the mechanical behaviour of this steel will be accurately described with constitutive laws that are currently under development. New experimental data in relation with Bauschinger effects must be obtained to implement a kinematic hardening law in the constitutive model. Model parameters will be validated with other experiments, such as in-plane shear tests on specially designed specimens [9]. It will allow us to interpret results of more complex experiments, e.g. the atypical crack path in shear cutting tests, and to develop and validate a failure criterion.

We managed to interrupt tearing and shear cutting experiments and succeeded in having stopped cracks. Little damage was detected from first observation of these specimens. Metallographic preparation must be improved in order to reveal damage in relation with the deformation microstructure.

6 References

[1] C. Scott, C. Guelton, S. Allain, M. Farat, The development of a new Fe-Mn-C austenitic steel for automotive application, La Revue de Métallurgie-CIT (2006) 293-302

[2] A. Dalloz, J. Besson, A.-F. Gourgues-Lorenzon, T. Sturel, A. Pineau, Effect of shear cutting on ductility of a dual phase steel, Engineering Fracture Mechanics, in press

[3] A. Bacha, D. Daniel, H. Klöcker, Metal ductility at low stress triaxiality application to sheet trimming, Journal of Materials Processing Technology 203 (2008) 480–497

[4] S. Allain, J.-P. Chateau, D. Dahmoun, O. Bouaziz, Modeling of mechanical twinning in high manganese content austenitic steel, Materials Science and Engineering A 387 (2004) 272-276

[5] E. Mahgoub, X. Deng, M. A. Sutton, Three-dimensional stress and deformation fields around flat and slant cracks under remote Mode I loading conditions, Engineering Fracture Mechanics 70 (2003) 2527–2542

[6] T. Pardoen, F. Hachez, B. Marchioni, P.H. Blyth, A.G. Atkins, Mode I fracture of sheets metal, Journal of the Mechanics and Physics of Solids 52 (2004) 423 – 452

[7] F. Bron, J. Besson, A. Pineau, A yield function for anisotropic materials: application to aluminium alloys, International Journal of Plasticity 20 (2004) 937-963

[8] S. Allain, P. Cugy, C. Scott, J.P. Chateau, A. Rusinek, A. Deschamps, Influence of the plastic instabilities on the mechanical properties of a high manganese austenitic FeMnC steel, International Journal of Materials Research 99 (7) (2008) 734-738

[9] M. Brünig, O. Chyra, D. Albrecht, L. Driemeier, M. Alves, A ductile damage criterion at various stress triaxialities, International Journal of Plasticity 24 (2008) 1731–1755